Multi-year ground-based observations of aerosol-cloud interactions in the Mid-Atlantic of the United States

Siwei Li[1*], Everette Joseph[1,2], Qilong Min[2] and Bangsheng Yin[2]

1. HOWARD UNIVERSITY

2355 6TH STREET NW WASHINGTON, DC 20059

*E–MAIL: SIWEI.LI@HOWARD.EDU

PHONE: 202-865-8678

2. ATMOSPHERIC SCIENCES RESEARCH CENTER, STATE UNIVERSITY OF NEW YORK AT ALBANY, ALBANY, NY 12203, USA

Multi-year ground-based observations of aerosol-cloud interactions in the Mid-Atlantic of the United States

Key words

Aerosols; aerosol-cloud interaction; cloud droplet effective radius; cloud optical depth; fine particles

Abstract

The U.S. Mid-Atlantic region experiences a wide variability of aerosol loading and frequent episodes of elevated anthropogenic aerosol loading associated with urban pollution conditions during summer months. In this study, multi-year ground-based observations (2006 to 2010) of aerosol and cloud properties from passive, active and in situ measurements at an atmospheric measurement field station in the Baltimore-Washington corridor operated by Howard University were analyzed to examine aerosol indirect effect on single-layer warm clouds including cloud optical depth (COD), liquid water path (LWP), cloud droplet effective radius (Re) and cloud droplet number concentration (N_d) in this region. A greater occurrence of polluted episodes and cloud cases with smaller Re ($<7\ \mu m$) were found during the polluted year summers (2006, 2007 and 2008) than the clean year summers (2009 and 2010). The measurements of aerosol particulate matter with aerodynamic diameter$\leq$2.5 μm (PM2.5) were used to represent the aerosol loading under cloudy conditions. Significant negative relationships between cloud droplet Re and PM2.5 were observed. Cloud cases were separated into clean and polluted groups based on the value of PM2.5. The cloud droplet Re was found proportional to LWP under clean conditions but weakly dependent on LWP under polluted conditions. The N_d was proportional to LWP under polluted condition but weakly dependent on LWP under clean conditions. Moreover, the effects of increasing fine aerosol particles on

modifying cloud microphysical properties were found more significant under large LWP than small LWP in this region.

1. Introduction

Investigation of the radiative forcing from aerosol-cloud interactions (RFaci) is crucial to estimates and interpretations of the Earth's changing energy budget (IPCC, 2013). The changes of cloud active aerosols can impact cloud microphysical properties, precipitation and the meteorological and radiance responses of clouds. A growing list of studies with space- and ground-based observations provides convincing evidences of RFaci. By using satellite remote sensing, Han et al. (1998) showed that cloud-droplet concentrations correlate to the cloud condensation nuclei (CCN) at different regions. Feingold et al. (2001) defined the ratio of logarithmic Re and aerosol optical depth (AOD) to represent the RFaci and Feingold et al. (2003, 2006) reported the observed RFaci by using ground-based observations of cloud and aerosol properties provided by the Atmospheric Radiation Measurement (ARM) at the Southern Great Plains (SGP) site in Oklahoma. Also with ARM SGP observations Kim et al. (2003, 2008, 2012) demonstrated the positive relationship between COD and LWP, an inverse relationship between Re and aerosol scattering coefficient and the role of adiabaticity in RFaci. Nzeffe et al. (2008) showed that Re reduced under polluted airmasses for given LWP based on the ground-based observations from Howard University Beltsville Campus (HUBC) facility.

However untangling aerosol effects on clouds and precipitation is still challenging. The extent to which aerosols impact clouds can be different or even opposite under different cloud regimes. The RFaci can be buffered by compensation between different cloud responses to aerosols (Rosenfeld et al., 2014, Stevens and Feingold, 2009). That explains why the statistical effects of aerosol on clouds and precipitation are not agreed upon. But the RFaci is still evident in specific circumstance or regimes (Stevens and Feingold, 2009, Huang et al., 2014 and Pan et al., 2015). The complexity

of the climate system and the inadequacy of measurements and methodologies have made it very challenging to obtain a more detailed understanding of aerosol-cloud interactions and their effects on climate (McComiskey and Feingold, 2012; Stevens and Feingold, 2009). Part of the challenge is reducing the uncertainty in estimates of RFaci, which as pointed out by McComiskey and Feingold (2012) requires small scale studies. Though field experiments that produce "process scale" observations of aerosol-cloud interaction continue to occur, historically they have been insufficient in number, regional diversity and duration. Current satellite-based sensors can provide global coverage and long-term measurements of aerosols and clouds. However detailed understanding of the RFaci is limited by the large scale, coarse time resolution and inherent limitations in the retrieval algorithms and sensors. Ground-based sensors can provide long-term measurements which are more accurate, stable, smaller scale and higher temporal resolution at specific region of interest compared to satellite sensors. A number of ground-based observation facilities (e.g. ARM sites) have been developed to study aerosol, clouds, precipitation and their influences on global climate change. Independent from ARM the HUBC station ($39.054\ ^{o}$ N and $76.877\ ^{o}$ W) was established for atmospheric measurements in the U.S. Mid-Atlantic region. This region experiences a wide variability of aerosol loading and frequent episodes of elevated anthropogenic aerosol loading associated with urban pollution conditions during summer months as seen in analyses of derived AOD from Aerosol Robotic Network (AERONET) and a collocated air quality monitoring operated by the Maryland Department of the Environment (MDE) (Holben et al., 1998). Thus, the observations of aerosol and cloud macro- and micro-physical properties in this region are valuable for investigating aerosol-cloud interaction and its impacts on weather and climate. Nzeffe et al. (2008) previously observed aerosol indirect effect based on six months of observations at HUBC site in 2005. This study extends their work to analysis five years (from 2006 to 2010) of ground-based observations of aerosol and cloud

properties for systematically investigating aerosol impacts on variability of cloud properties including COD, LWP, Re and Nd during summer in this region.

2. Measurements

The HUBC facility in Beltsville, MD is situated in a rural-suburban transition region between Washington, DC and Baltimore, MD urban centers. It has a wide range of sensors deployed to observe atmospheric radiation, surface fluxes, aerosol, cloud properties and other climate and weather processes (Nzeffe et al., 2008).

Among the sensor observations, LWP is determined from a dual frequency (23.8 and 31.4 GHz) Microwave radiometer (MWR) (Westwater et al., 2001). The error of the MWR LWP retrieval consists of instrument error, errors associated with the climatological profiles used for the retrieval (given day to day variability of atmospheric temperatures from this climatology), and errors from the absorption model used to develop parameters for the retrieval algorithm (Turner et al., 2007). The errors associated with instrument and climatological profiles used are considered random errors and thus are minimized with increasing sample size of data. The error associated with absorption model is considered a systematic bias and represents the preponderance of the total error. Instrument uncertainty and retrieval errors associated with the climatological profiles and the microwave absorption model results in a total uncertainty of retrieved LWP around 20 g/m^2 (Turner et al., 2007) but the consequence of the systematic error is minimized while relative differences are investigated (e.g cloud droplet Re vs. LWP).

AOD is measured with a MultiFilter Rotating Shadowband Radiometer (MFRSR) which is a sensor with a shading band that rotates, measuring global downwelling irradiance, diffuse irradiance and direct beam irradiance calculated from global and diffuse irradiance. More detail on the instrument design can be found in Harrison et al., (1994). The MFRSR is calibrated using data acquired on clear sky days via the Langley regression which is based on linear regressions of the log of direct beam

irradiance versus airmass and the calibration constant I_0 is used to compute transmittances during cloudy conditions (Harrison et al., 1994; Harrison and Michalsky, 1994). The AOD is retrieved based on the algorithm developed by Harrison and Michalsky (1994). For quality control, the retrieved AOD is compared with AERONET observation at NASA Goddard Space Flight Center (GSFC), around 5 miles southeast of the HUBC facility. High correlation coefficient (0.94) is found between them during the study period (from 2006 January to 2010 December).

However retrieval of AOD is not available from any passive remote sensor during cloud periods, so hourly in situ measurements of particulate matter with aerodynamic diameter ≤ 2.5 μm (PM2.5) are obtained from samplers operated by the MDE at the HUBC site to estimate aerosol loading under cloudy conditions. Although surface PM2.5 is related more to small particles within boundary layer while AOD presents the total column aerosol loading, surface PM2.5 had a good correlation with AOD in the District of Columbia-Maryland area based on the study of PM2.5-AOD relationship in the United States (Liu et al., 2004). We also found that the measured PM2.5 has a significant positive relationship with MFRSR retrieved AOD with correlation coefficient of 0.63 during clear-sky conditions in summer as seen in Fig. 1.

In situ aerosol size distributions are measured by a Fast Mobility Particle Sizer (FMPS) which was developed based on electrical aerosol spectrometer technology from Tartu University (Tammet et al. 2002; TSI 2006). The FMPS measures particle size distributions in the range from the 6 nm to 560 nm with 16 channels per decade every second. However the FMPS measurements at HUBC are only available during the NASA DISCOVER-AQ (a field campaign for deriving information on surface conditions from column and vertically resolved observations relevant to air quality) field campaign in the Baltimore-Washington, D.C., area, in July 2011. So two days of FMPS observations under clear sky with different aerosol loading (polluted day, July 20th, 2011 and clean day, July 14th, 2011) are used to illustrate the differences of detail aerosol size distributions between clean and polluted days in this study.

A family of retrieval algorithms has been developed for COD and cloud droplet Re retrievals based on MFRSR and MWR (Min and Harrison, 1996; Min et al, 2001; Min et al, 2004, Wang and Min, 2008, Wang and Huang, 2009). Cloud droplet optics is parameterized in terms of average Re and total LWP based on MIE theory (Slingo, 1989; Hu and Stamnes, 1993). COD is retrieved by a Nonlinear Least Squares Method through iterative procedure (Min and Harrison, 1996; Min et al, 2004). Cloud droplet Re is simultaneously retrieved with total LWP observed from MWR while Re is assumed equal to 8 μm when measurement of total LWP is not available. The retrieved Re is an equivalent vertically uniform parameter ("mean Re"). Compared with eight aircraft in situ vertical profiles (obtained from measurements of Forward Spectra Scattering Probe), the retrieved Re for single-layer warm water clouds agree well with in situ measurements, within 5.5% (Min et al., 2003). It was shown that a 13% (LWP, 20 g/m^2) uncertainty in observed liquid water path can result in 12.7% difference in inferred cloud effective radius, on average but only 1.5% difference in retrieved cloud optical depth. The uncertainty of the LWP measured by MWR is mainly systematic biases (Turner et al., 2007). But the consequence of LWP bias is minimized when considering that the relative difference of Re vs. LWP for clear and polluted conditions is our interest in this study for investigating the RFaci. With the assumption that the clouds in question are adiabatic and N_d is vertically constant, the N_d is obtained from a parameterization in terms of COD and Re (Boers et al., 2006; Bennartz, 2007; Min et al., 2012). Through comparing N_d calculated from Moderate Resolution Imaging Spectroradiometer (MODIS) measured COD and Re to in-situ measured N_d Min et al. (2012) showed that there was a high correlation between retrieved N_d and in situ measurements with a correlation coefficient of about 0.91.

Up to three layers cloud-base height were provided by a Vaisala CT25k ceilometer. The CT25k ceilometer is equipped with a pulsed near-infrared diode laser (905 nm) which is located at the site within the vicinity of the MFRSR. The measurement range of this CT25k ceilometer is from 0 to 7500 m and the vertical resolution is 30 m.

Retrieval of aerosol extinction coefficients from Mie scattering lidar is improved recently (Li et al., 2015). However the accuracy of aerosol extinction coefficient retrieval from low power lidar CT25K is still challenging and needs more investigation and validation. So in this paper we use surface measurements of PM2.5 instead of AOD.

This investigation is limited to summer months (June, July and August) because the U.S. Mid-Atlantic region experiences the largest variation of aerosol loading due to episodic summertime pollution events. Strong convection that occurs during summer results in more boundary layer clouds, which are tightly coupled with surface aerosols. The inter-seasonal variation of aerosol loading is also large but so is the variation of dynamical and thermodynamic conditions that dominate cloud micro- and macro- physical properties. The latter effect on cloud properties could complicate the analysis of aerosol cloud interaction on this scale. For this reason the study is confined to the summer months. Since the domain of the field of view of an upward looking MFRSR is about a couple of kilometers under lower level cloud condition (Min et al., 2001), following Min et al. (2003) and Nzeffe et al. (2008), cloud properties retrieved from MFRSR are 5 minutes averaged and only those cases of single-layer clouds continuously lasting longer than 30 minutes were used for this study. To increase the likelihood that the aerosols at the cloud base can be represented by the surface measurements, we confine the observations to low clouds with cloud base height is lower than 3 km. For optical thin clouds the radiative flux is sensitive to the small changes of LWP (Min and Duan, 2005) and consequently the Re retrieved from combination of MWR LWP and MFRSR COD has relatively larger uncertainties, mainly due to the uncertainty of MWR measurements (Min et al., 2003). So cases with LWP smaller than 40 g/m^2 are removed in the data analysis for this study. Clear sky and broken clouds are also removed by using MFRSR measured direct beam (derived total optical depth smaller than 5), MFRSR estimated cloud-fraction (smaller than 90%) (Min et al., 2008) and ceilometer undetected clouds. Possible precipitation are avoided by screening clouds with LWP>180 g/m^2,

Re>15 μm andceilometer detected rain/cloud near surface (lower than 30 m). Ceilometer derived cloud layers and cloud base height are used to screen out high clouds (higher than 3km) and possible multi-layer clouds. In the summer of this region air temperature is usually around $0\ ^{o}C$ at the height of 5 km and above $-10\ ^{o}C$ at the height of 6 km at daytime from radiosonde measurements. Cloud top heights are seldom higher than 6 km when cloud base height is below 3 km except for those deep convective clouds which are already removed in this study through the threshold of LWP. So the ice particles contamination can be neglected.

3. Results and discussion

3.1 Comparison of aerosol, cloud properties in polluted and clean years

Based on the daily average AOD, the summer average AOD in years 2006-2010 were 0.50, 0.60, 0.40, 0.35, and 0.36, respectively, (Fig. 2a). The probability distribution of daily AOD shows that more frequent episodes of high aerosol loading (AOD>0.50) occur during the summers of year 2006, 2007 and 2008 as compared to those in year 2009 and 2010 (figure 2b). The measurements of PM2.5 from MDE at HUBC site show that the average PM2.5 values in the summer of year 2006, 2007 and 2008 are 20, 20.5 and 18 μg/m^3 respectively which are larger than that in the summers of year 2009 and 2010 (14 and 16μg/m^3 respectively) (figure 2c). Figure 2d shows that a greater occurrence of polluted cases (PM2.5 larger than 30 μg/m^3) occur in year 2006, 2007 and 2008 compared to that in year 2009 and 2010. Thereafter the year 2006, 2007 and 2008 are denoted as polluted years while the year 2009 and 2010 are denoted as clean years for convenience.

The retrievals of AOD are commonly based on measurements of spectral extinction of solar radiation due to aerosol scattering and absorption in the atmospheric column. Passive instrument, such as the MFRSR, cannot readily discern AOD from COD under cloudy conditions. So in this study the synchronous PM2.5 measurements are used to represent the aerosol situation under clouds given that AOD measurements are not available under cloudy condition. There are a total of 9

250 cloudy or partly cloudy days for which low single-layer clouds lasting longer than 30
251 minutes with PM2.5 larger than 20 μg/m^3 are observed and 11 similar days with
252 PM2.5 smaller than 20 μg/m^3 in polluted year summers. The 20 μg/m^3 is chosen
253 based on mean value and number of cases in polluted years. For similar 23 days in
254 clean year summers, PM2.5 are smaller than 20 μg/m^3 for all cloud cases. The
255 average PM2.5 under cloudy conditions in the polluted years is about 24.8 μg/m^3
256 while it is only 11.1 μg/m^3 in the clean years. The probability distribution shows that
257 there are more than 60% cloud cases with surface PM2.5 value larger than 20 μg/m^3
258 in the polluted years while there is no cloud case with PM2.5 value larger than 20
259 μg/m^3 found in the clean years (figure 3a). The average LWP for clouds in the
260 polluted years (124.51 g/m^2) is around 10% larger than that in clean years (114.53
261 g/m^2) and that is due to the more frequent cases of LWP larger than 150 g/m^2 (figure
262 3b). The average COD in the polluted years (25.37) is about 25% larger than that in
263 the clean years (20.39). There are about 25% cloud cases with COD larger than 30 in
264 the polluted years while there are only 7% cloud cases with COD larger than 30 in
265 the clean years (figure 3b). In the polluted years the distribution of Re shifts to the
266 smaller value and the average Re (7.97 μm) is about 13% smaller compared to that in
267 the clean years (9.12 μm).
268 To assess the difference of microphysical properties of clouds with same LWP during
269 the polluted and clean years, the COD and Re values are sorted into 7 bins of LWP
270 with 20 g/m^2 bin widths. The mean COD and Re are computed and plotted with the
271 arithmetic mean of each bin. Error bars represent the 95% confidence levels of the
272 mean value. Over the entire LWP range, the mean COD observed during the polluted
273 years is larger than that during the clean years by as much as 5 (Fig. 4a) and the
274 mean Re is less during the polluted years than that during the clean years by as much
275 as 1.2 μm(Fig. 4b). The mean COD and Re increase with increasing LWP during both
276 the polluted and clean years and the differences of the mean COD, Re during the
277 polluted and clean years (COD polluted – COD clean, Re clean - Re polluted) are also
278 increased with increasing of LWP.

279

280 3.2 Aerosol indirect effects

281 To investigate aerosol indirect effects on cloud microphysical properties, the
282 measurements of Re are plotted along with the value of PM2.5 in figure 5a. Figure 5a
283 shows a negative relationship between Re and PM2.5 with the correlation coefficient
284 of -0.382 for the entire 5 year summer observations. Individually, the relationships of
285 Re and PM2.5 in polluted years and clean years are all negative with the correlation
286 coefficient of -0.285 and -0.197 respectively (figure 5b, c). The correlations are all
287 statistical significant through T-test analysis (Wilks, 1995). The entire 5 year summer
288 observations are segregated into clean group (PM2.5 < 20 μg/m^3, number of data:
289 631) and polluted group (PM2.5 >= 20 μg/m^3, number of data: 367). The observed
290 pairs of Re and LWP are shown in Figure 6a for clean and polluted groups. It is shown
291 that Re increases with increasing LWP under clean conditions while Re deceases with
292 increasing LWP under polluted condition. When LWP is large (>120 g/m^2) the Re
293 is much larger under clean conditions than under polluted conditions for most cases.
294 When LWP is small (<100 g/m^2) the Re is similar or even smaller under clean
295 conditions than under polluted conditions. Cloud droplets compete with each
296 other as they grow through water diffusion. There is less competition among
297 droplets at lower cloud condensation nuclei (CCN) concentration and thus a wider
298 spectrum of droplets is activated. This is in contrast to higher CCN concentration
299 where the increased competition limits the spectral range of droplet activation.
300 Figure 6a shows that there is a significant positive relationship between N_d and
301 LWP with correlated coefficient of 0.612 under polluted conditions and a slightly
302 negative relationship with correlated coefficient of -0.15 under clean conditions.
303 Under clean conditions aerosol particle number concentration (N_a) is less, most
304 aerosol particles are activated into cloud droplets with sufficient water supply which
305 means N_d is limited by N_a, so N_d is nearly independent of LWP and the droplet
306 growth process dominates in the development of cloud. On the other hand, under

polluted conditions with abundant N_a, there are more potential aerosol particles that can be activated into cloud droplets with sufficient water supply and strong updraft velocity. So the N_d is observed increasing with increasing LWP under polluted conditions. Larger number of activated droplets increase cloud droplet concentration but then cause relatively small Re due to the increased competition for available water vapor. It is also noticed that the N_d under polluted conditions is larger than under clean condition for most cases when LWP is large (larger than 120 g/m^2) but is similar or even smaller than that under clean conditions when LWP is small (smaller than 100 g/m^2). Those are consistent with the aerosol-limited regime and updraft-limited regime from the study by Reutter et al., (2009) which simulated cloud droplet formation under different regimes based fine aerosol particles. In the aerosol-limited regime that is characterized by a relative high updraft velocity and water vapor supersaturation which implies large LWP, N_d is directly proportional to N_a. The high updraft velocity and water vapor supersaturation can activate nearly all aerosol particles. In the updraft-limited regime that is characterized by relative low updraft velocity and water vapor supersaturation which implies small LWP, N_d is weakly dependent on N_a. Under extreme conditions with very low updraft velocity but very large N_a, supersaturation can be quenched by the cost of water taken by aerosol particles. So the N_d could be smaller under polluted conditions than that under clean conditions when LWP is small. Through cloud parcel model simulation, Reutter et al. (2009) indicated that the variability of N_a in the Aitken and accumulation mode mostly dominates the variability of initial N_d except at low supersaturations in updraft limit regimes.

To know aerosol size under polluted condition in this region, the in situ observations of aerosol size distributions from a FMPS at HUBC during DISCOVER AQ field

campaign under clean and polluted conditions in this region are compared (Fig. 7). On a polluted day (July 20th , 2011), the total number concentration of aerosol is much higher than that on a clean day (July 14th, 2011) and it is almost entirely due to the higher number concentration of aerosol particles in Aitken and accumulation mode. Although the field campaign only last one month at HUBC the detailed aerosol size distributions observation gave us a sense that the increase of aerosol particles in this area may be mainly due to the increase of fine particles. Aerosol optical properties are related to aerosol size distribution. As an aerosol size indicator, aerosol angstrom coefficient generally decreases with increasing aerosol size. The long-term observations show that the observed hourly angstrom coefficients which are calculated from MFRSR measured AOD at 415nm and 860nm have significant positive relationship (P<0.0001) with hourly PM2.5 (Fig. 8). This correlation implies that an increase of PM2.5 value is associated with an increase of total column fine particles over this region given that angstrom coefficient is calculated from column AOD at different wavelength.

In the updraft-limited regime with low supersaturations, supersaturation can be quenched by the cost of water taken by large amount of fine aerosol particles. So the N_d under polluted conditions for which fine aerosol particles dominate appears to be similar or even smaller than the N_d under clean conditions when LWP is small (smaller than 100 g/m^2 in this study). Within the aerosol-limited regime with large updraft velocity and supersaturation, N_d is larger under polluted condition because more aerosol particles can be activated to cloud droplets.

4. Conclusions

Long-term ground-based observations of aerosol and cloud optical properties from HUBC facility are employed to show aerosol impacts on cloud properties in the Mid-Atlantic in the United States. The retrieved AOD at the HUBC site agrees well

360 with that from a nearby AERONET site and closely correlates with PM2.5 measured
361 at the site. The distributions of daily mean AODs and PM2.5 show that there were a
362 greater occurrence of polluted episodes in year 2006, 2007 and 2008 as compared to
363 year 2009 and 2010. The statistical analysis of collocated measurements of PM2.5
364 and cloud properties shows that in the polluted years there are more cloud cases
365 with larger PM2.5 values, smaller Re and larger COD. Within the same LWP bins, the
366 mean COD is evidently larger and the mean Re is smaller in the polluted years. The
367 Re is found inversely related to PM2.5 with correlated coefficient of -0.285 and
368 -0.197 in polluted years and clean years respectively. For all cases, the correlation
369 coefficient between Re and PM2.5 is -0.382. The entire 5 year summer observations
370 of cloud properties are segregated into polluted and clean groups based on PM2.5
371 value (>= 20 μg/m^3, <20 μg/m^3 respectively). The variability of Re and N_d with
372 increasing LWP are found different under polluted and clean conditions. Under
373 polluted conditions, Re slightly deceases with increasing LWP while N_d significantly
374 increases with increasing LWP. Under clean conditions, Re increases with increasing
375 LWP while N_d is nearly independent of LWP. The N_d is larger under polluted
376 conditions than that under clean conditions when LWP is large (>120 g/m^2) but
377 similar or even smaller than that under clean conditions when LWP is small (<100
378 g/m^2). Simulations done by Reutter et al., (2009) suggest this phenomenon is
379 consistent with that fine aerosol particles impacts on N_d in aerosol-limit regime with
380 high supersaturation and in updraft-limit regime with low supersaturation (Reutter
381 et al., 2009). The measurements of aerosol size distribution and angstrom coefficient
382 show that the increase of aerosol particles in the summer of Baltimore-Washington,
383 DC region is mainly due to the increase of fine particles. Under clean conditions, the
384 N_d is limited by N_a, so increasing LWP is mainly attributed to droplet growth. Under
385 polluted conditions, more new cloud droplets can be activated with high
386 supersaturation and the increase of N_d dominates over cloud droplets growth. But

with lower supersaturation, abundant aerosol particles would take up water and supersaturation could be reduced to a level which prevents activation of cloud droplets from fine (Aitken and accumulation) mode aerosol particles. So the N_d and Re are strongly impacted by N_a in fine mode under high supersaturation but weakly impacted by N_a in fine mode under lower supersaturation. Analysis based on the long-term observations including diverse dynamical and aerosol regimes at HUBC site can provide climate assessment of RFaci in the mid-Atlantic corridor, where frequent severe pollution episodes occur.

Acknowledgements: This work is supported by the National Oceanic and Atmospheric Administration, Educational Partnership Program, U.S. Department of Commerce, under Agreement No. NA11SEC4810003.

References

Ackerman AS, Kirkpatrick MP, Stevens DE, and Toon OB. 2004. The impact of humidity above stratiform clouds on indirect aerosol climate forcing, *Nature*, **432**, 1014–1017, doi:10.1038/nature03174.

Albrecht BA. 1989. Aerosol, cloud microphysics, and fractional cloudiness, *Science*, **245**, 1227–1230, doi:10.1126/science.245.4923.1227.

Brioude J., et al. 2009. Effect of biomass burning on marine stratocumulus clouds off the California coast, *Atmos. Chem. Phys* ., **9** , 8841 – 8856, doi: 10.5194/acp-9-8841-2009.

Bennartz R. 2007. Global assessment of marine boundary later cloud droplet number concentration from satellite, *J. Geophys. Res.*, **112**, D02201, doi: 10.1029/2006JD007547.

Boers R, Acarreta JA, Gras JL. 2006. Satellite monitoring of the first indirect aerosol effect: Retrieval of the droplet con-centration of water clouds, *J. Geophys. Res.*, **111**, D22208, doi:10.1029/2005JD006838.

Coakley JA, Walsh CD. 2002. Limits to the aerosol indirect radiative effect derived from observations of ship tracks, *J. Atmos. Sci.* , **59**, 668 –680, doi: http://dx.doi.org/10.1175/1520-0469(2002)059<0668:LTTAIR>2.0.CO;2

Feingold G, Remer LA, Ramaprasad J, Kaufman YJ. 2001. Analysis of smoke impact on clouds in Brazilian biomass burning regions: An extension of Twomey's approach, *J. Geophys. Res.*, VOL. **106**, NO. D19, PAGES 22,907–22,922

Feingold G, Eberhard W, Veron D, Previdi M. 2003. First measurements of the Twomey indirect effect using ground-based remote sensors, *Geophys. Res. Lett.*, **30**(6), 1287, doi:10.1029/2002GL016633.

Feingold G, Furrer R, Pilewskie P, Remer LA, Min Q, Jonsson H. 2006. Aerosol indirect effect studies at southern Great Plains during the May 2003 intensive operations period, *J. Geophys. Res.*, **111**, D05S14, doi:10.1029/2004JD005648.

Han Q, Rossow WB, Lacis AA. 1994. Near global survey of effective droplet radii in liquid water clouds using ISCCP data. *J. Climate*, **7**, 465–497.

Han Q, Rossow WB, Chou J, Welch RM. 1998. Global variation of cloud effective droplet concentration of low-level clouds. *Geophys. Res. Lett.*, **25**, 1419–1422.

Harrison L, and Michalsky J. 1994. Objective algorithms for the retrieval of optical depths from ground-based measurements, *Appl. Opt.*, **33**, 5126 – 5132.

Harrison L, Michalsky J, Berndt J. 1994. Automated multifilter rotating shadow-band radiometer: An instrument for optical depth and radiation measurements, *Appl. Opt.*, **33**, 5118 – 5125.

Holben BN, Eck TF, Slutsker I, Tanré D, Buis JP, Setzer A, Vermote E, Reagan JA, Kaufman YJ, Nakajima T, Lavenu F, Jankowiak I, Smirnov A. 1998. AERONET-A federated instrument network and data archive for aerosol characterization, *Remote Sens. Environ.*, **66** ,1 – 16.

Hu, Y. X., and K. Stamnes, An accurate parameterization of the radiative properties of water clouds suitable for use in climate models, *J. Clim*., 6, 728– 742, 1993.

Huang J., T. Wang, W. Wang, Z. Li, and H. Yan. 2014. Climate effects of dust aerosols over East Asian arid and semiarid regions, J. *Geophys. Res. Atmos*., 119, 11,398–11,416, doi:10.1002/2014JD021796.

Kim BG, Schwartz SE, Miller MA, Min Q. 2003. Effective radius of cloud droplets by ground-based remote sensing: Relationship to aerosol, *J. Geophys. Res.*, **108**(D23), 4740, doi:10.1029/2003JD003721.

Kim BG, Miller MA, Schwartz SE, Liu Y, Min Q. 2008. The role of adiabaticity in the aerosol first indirect effect, *J. Geophys. Res.*, **113**, D05210, doi:10.1029/2007JD008961.

Kim Y, Kim B, Miller M, Min Q, Song C. 2012. Enhanced aerosol-cloud relationships in more stable and adiabatic clouds, *Asia-Pacific Journal of Atmospheric Sciences*, **48**, Issue 3, pp 283-293, doi: 10.1007/s13143-012-0028-0

Lebsock MD, Stephens GL, Kummerow C. 2008. Multisensor satellite observations of aerosol effects on warm clouds, *J. Geophys. Res.*, **113**, D15205, doi:10.1029/2008JD009876.

Lee SS, Penner JE, Saleeby SM. 2009. Aerosol effects on liquid-water path of thin stratocumulus clouds, *J. Geophys. Res.*, **114**, D07204, doi:10.1029/2008JD010513.

Li C, Pan Z, Mao F, Gong W, Chen S, Min Q. 2015. De-noising and retrieving algorithm of Mie lidar data based on the particle filter and the Fernald method. *Opt Express*. 2015 Oct 5;23(20):26509-20, doi: 10.1364/OE.23.026509.

Liu, Y., Park, R. J., Jacob, D. J., Li, Q. B.; Kilaru, V., Sarnat, J. A. 2005. Mapping annual mean ground-level PM2.5 concentrations using Multiangle Imaging Spectroradiometer aerosol optical thickness over the contiguous United States. J. Geophys. Res, **109**, D22206, doi: 10.1029/2004JD005025.

McComiskey A., Feingold G. 2012. The scale problem in quantifying aerosol indirect effects, *Atmos. Chem. Phys.*, **12**, 1031-1049, doi:10.5194/acp-12-1031-2012.

Min Q, Harrison L. 1996. Cloud properties derived from surface MFRSR measurements and comparison with GOES results at the ARM SGP site, *Geophys. Res. Lett.* , **23** , 1641 – 1644.

Min, Q., L. C. Harison, and E. Clothiaux (2001), Joint statistics of photon path length and cloud optical depth: Case studies, J. Geophys. Res., 106, 7375–7386.

Min Q, Duan M, Marchand R. 2003. Validation of surface retrieved cloud optical properties with in situ measurementsat the Atmospheric Radiation Measurement Program (ARM) South Great Plains site, *J. Geophys. Res.*, **108**(D17), 4547,doi:10.1029/2003JD003385, 2003.

Min Q, Duan M. 2005. Simultaneously retrieving cloud optical depth and effective radius for optically thin clouds, *J. Geophys. Res.*, **110**, D21201, doi:10.1029/2005JD006136.

Min, Q., T. Wang, C. N. Long, and M. Duan. 2008, Estimating fractional sky cover from spectral measurements, *J. Geophys. Res*., 113, D20208, doi:10.1029/ 2008JD010278.

Min Q, Joseph E, Lin Y, Min L, Yin B, Daum PH, Kleinman LI, Wang J, Lee YN. 2012. Comparison of MODIS cloud microphysical properties with in-situ measurements over the Southeast Pacific, *Atmos. Chem. Phys.*, **12**, 11261–11273, www.atmos-chem-phys.net /12/11261/2012/doi:10.5194/acp-12-11261-2012

Nzeffe F., Joseph E, Min Q. 2008. Surface-based observation of aerosol indirect effect in the Mid-Atlantic region, *Geophys. Res. Lett.*, **35**, L22814, doi: 10.1029/2008GL036064.

Pan Z., W. Gong, F. Mao, J. Li, W. Wang, C. Li, and Q. Min. 2015, Macrophysical and optical properties of clouds over East Asia measured by CALIPSO, *J. Geophys. Res*. Atmos., 120, 11,653–11,668, doi:10.1002/2015JD023735.

Rosenfeld D, Sherwood S, Wood R, Donner L. 2014. Climate effects of aerosol-cloud interactions. *Science* **343**:379–380.

Rogers RR, Yau, MK. 1989. *A Short Course in Cloud Physics*, Int. Ser. Nat. Philos, 113: 290.

Slingo, A., A GCM parameterization for the shortwave radiative properties of water clouds, J. Atoms. Sci., 46, 1419–1427, 1989.

Stevens B, Feingold G. 2009. Untangling aerosol effects on clouds and precipitation in a buffered system, *Nature*, **461** , doi:10.1038/nature08281.

Storelvmo T, Kristjánsson JE, Myhre G, Johnsrud M, Stordal F. 2006. Combined observational and modeling based study of the aerosol indirect effect, *Atmos. Chem. Phys.*, **6**, 3583-3601, doi:10.5194/acp-6-3583-2006.

Tammet, H., Mirme, A., and Tamm, E. 2002. Electrical Aerosol Spectrometer of Tartu University, Atmos. Res. 62:315–324.

TSI. 2006. Fast Mobility Particle Sizer Spectrometer; Operation and Service Manual, TSI Incorporated, Shoreview, MN, USA.

Turner DD, Vogelmann AM, Johnson K, Miller M, Austin RT, Barnard JC, Flynn C, Long C, McFarlane SA, Cady-Pereira K, Clough SA, Chiu JC, Khaiyer MM, Liljegren J, Lin B, Minnis P, Marshak A, Matrosov SY, Min Q, O'Hirok W, Wang Z, Wiscombe W. 2007.Thin liquid water clouds: Their importance and our challenge. *Bull. Am. Meteorol. Soc.*, **88**(2), 177-190.

Twohy CH, Petters MD, Snider JR, Stevens B, Tahnk W, Wetzel M, Russell L, Burnet F. 2005. Evaluation of the aerosol indirect effect in marine stratocumulus clouds:

556 Droplet number, size, liquid water path, and radiative impact, *J. Geophys. Res.*, **110**,
557 D08203, doi:10.1029/2004JD005116.
558
559 Twomey S. 1974. Pollution and the planetary albedo, *Atmos. Environ.*, **8**, 1251– 1256.
560
561 Twomey S. 1977. Influence of pollution on shortwave albedo of clouds. *J. Atmos. Sci.*,
562 **34**, 1149–1152.
563
564 Wang T and Q. Min. 2008. Retrieving optical depths of optically thin and
565 mixed-phase clouds from MFRSR measurements, *J. Geophys. Res*. 113, D19203
566 Wang T and J. Huang . 2009. A method for estimating optical properties of dusty
567 cloud, *Chin. Opt. Lett*., 7(5), 368–372, doi:10.3788/COL20090705.0368
568
569 Westwater ER, Han Y, Shupe MD, Matrosov SY. 2001. Analysis of integrated cloud
570 liquid and precipitable water vapor retrievals from microwave radiometers during
571 the Surface Heat Budget of the Arctic Ocean project, *J. Geophys. Res.*, **106**, 32,019 –
572 32,030.
573
574 Wilks DS. 1995. *Statistical Methods in the Atmospheric Sciences*, Academic, San
575 Diego, Calif.
576
577 Wood R, Hartmann DL. 2006. Spatial variability of liquid water path in marine
578 boundary layer clouds: The importance of mesoscale cellular convection. *J. Climate*,
579 **19**, 1748–1764.
580
581 Zheng X, Albrecht B, Minnis P, Ayers K, Jonson H. 2010. Observed aerosol and liquid
582 water path relationships in marine stratocumulus, *Geophys. Res. Lett.*, **37**, L17803,
583 doi:10.1029/2010GL044095.
584
585
586

587

588

589

590

591

592

593 **Figure captions**

594

595 **Fig. 1**. The relationship of hourly average AOD and PM2.5 based on 5 years (2006 to
596 2010) summer time clear sky measurements.

597 **Fig. 2.** The aerosol properties for each year. (a)Summer averaged AOD with standard
598 deviation; (b) distribution of daily AOD measurements (bins: interval is 0.1 when
599 AOD is from 0 to 1.0 and the last bin is AOD >=1.0); (c) summer averaged PM2.5 with
600 standard deviation and (d) distribution of hourly PM2.5 measurements (bins: interval
601 is 5μm when PM2.5 is from 0 to 30 $\mu g / m^3$ and the last bin is PM2.5 >=30 $\mu g / m^3$).

602 **Fig. 3.** The distributions of PM2.5 and cloud properties during polluted years and
603 clean years. (a) PM2.5; (b)LWP ; (c) COD and (d)Re.

604 **Fig. 4.** The comparison of mean COD, mean Re between during polluted and clean
605 years. (a) Mean COD VS. LWP, (b) mean Re VS. LWP. Error bars represent the 95%
606 confidence level.

607 **Fig. 5.** (a) The relationship between Re and PM2.5. (a)For entire five years; (b)for
608 polluted years and (c)for clean years.

609 **Fig. 6.** (a) The relationship between Re and LWP under different PM2.5 value , and (b)
610 the relationship between cloud droplets number concentration and liquid water
611 path under different PM2.5 value.

612 **Fig. 7.** FMPS measured aerosol size distribution on the polluted day (July 20th, 2011)
613 and clean day (July 14th , 2011) during DISCOVER AQ field campaign.

614 **Fig. 8.** The relationship of 5 years summer time hourly average Angstrom coefficient
615 and PM2.5.

616

617

618 **Figures**

619 **Fig. 1.**

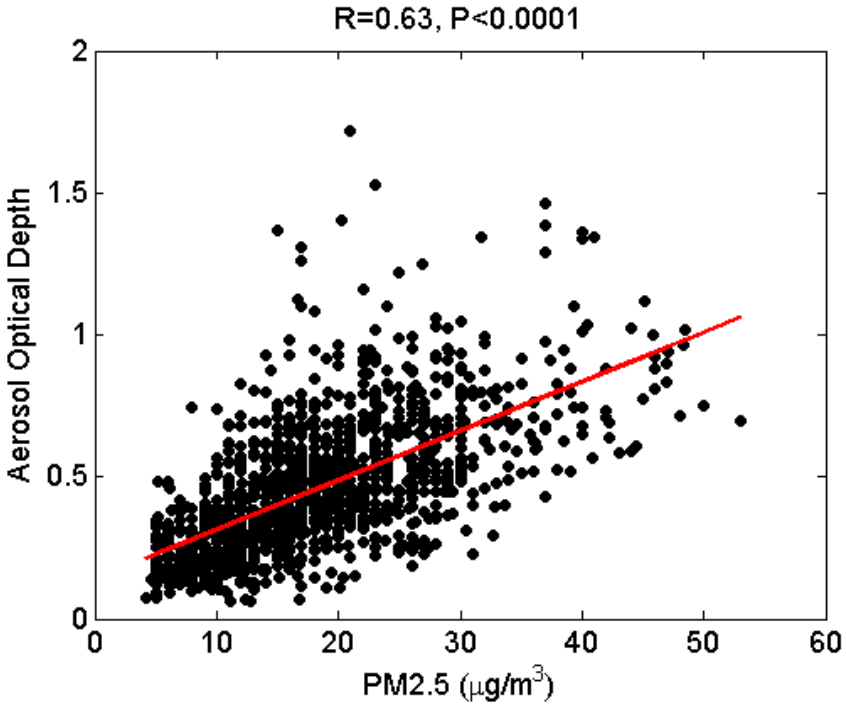

620

621 **Fig. 1**. The relationship of hourly average AOD and PM2.5 based on 5 years (2006 to
622 2010) summer time clear sky measurements.

623

624

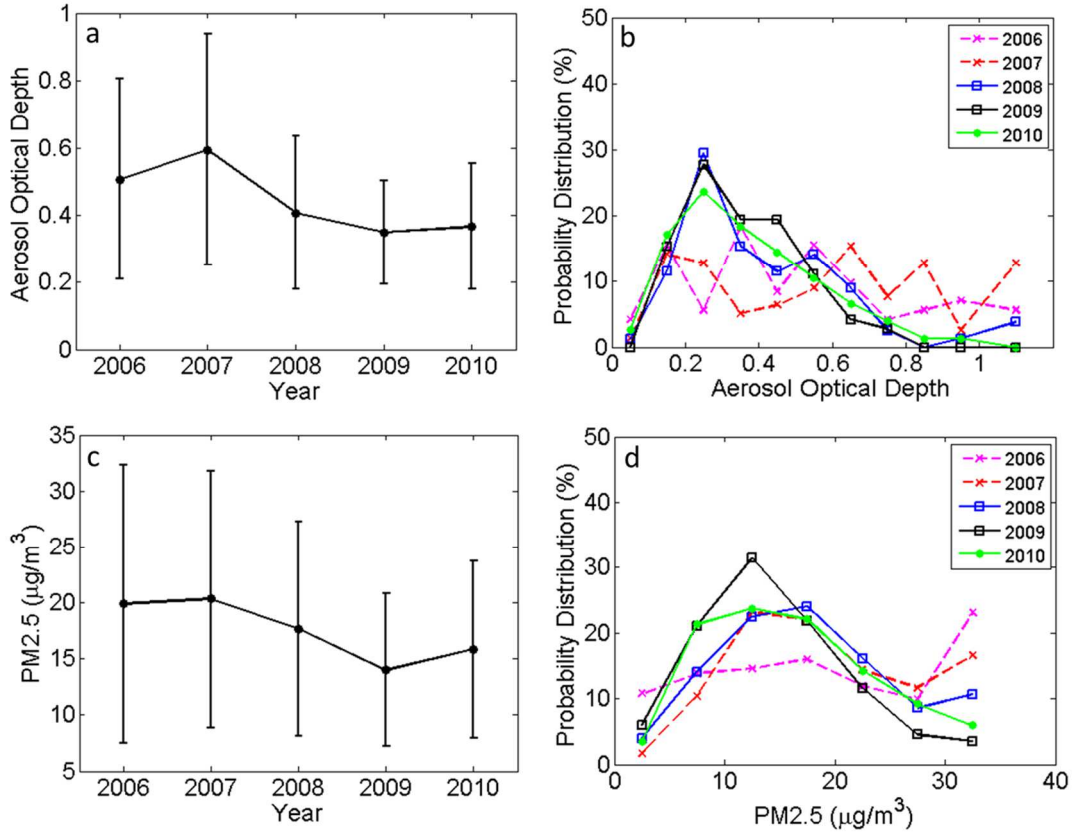

625

626 **Fig. 2.** The aerosol properties for each year. (a)Summer averaged AOD with standard
627 deviation; (b) distribution of daily AOD measurements (bins: interval is 0.1 when
628 AOD is from 0 to 1.0 and the last bin is AOD >=1.0); (c) summer averaged PM2.5 with
629 standard deviation and (d) distribution of hourly PM2.5 measurements (bins: interval
630 is 5μm when PM2.5 is from 0 to 30 $\mu g / m^3$ and the last bin is PM2.5 >=30 $\mu g / m^3$).

631

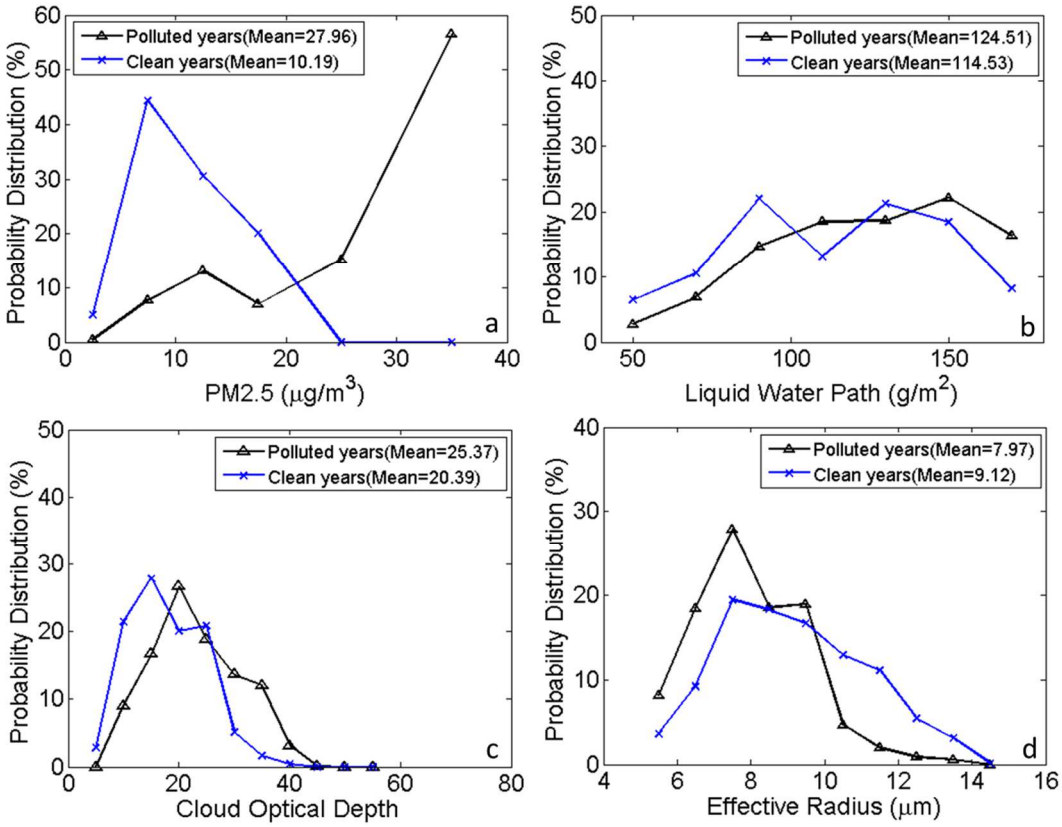

632

633 **Fig. 3.** The distributions of PM2.5 and cloud properties during polluted years and

634 clean years. (a) PM2.5; (b)LWP; (c) COD and (d)Re.

635

636

637

638

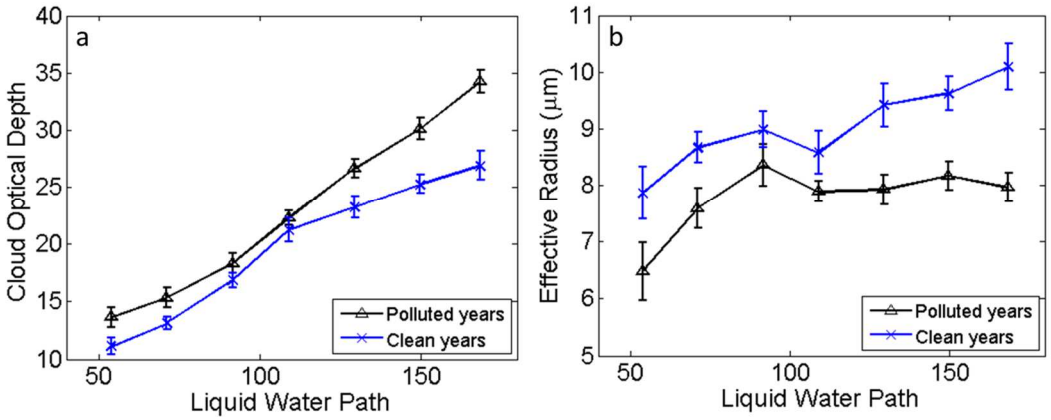

639

640 **Fig. 4.** The comparison of mean COD, mean Re between during polluted and clean
641 years. (a) Mean COD VS. LWP, (b) mean Re VS. LWP. Error bars represent the 95%
642 confidence level.

643

644

645

646

647

648

649

650

651

652

653 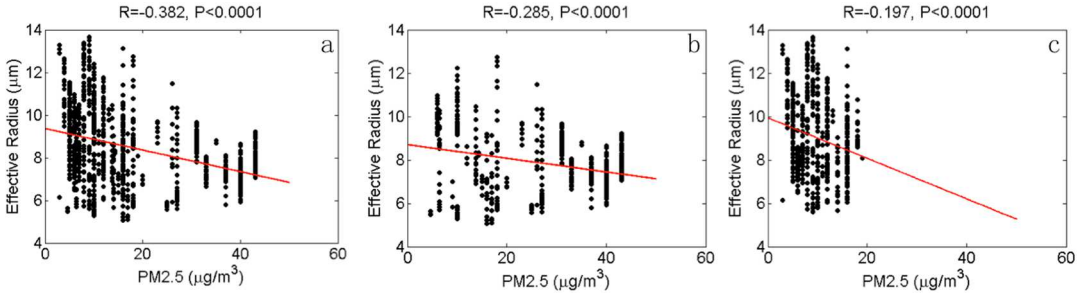

654 **Fig. 5.** The relationship between Re and PM2.5. (a)For entire five years; (b)for
655 polluted years and (c)for clean years.

656

657

658

659

660

661

662

663

664

665

666

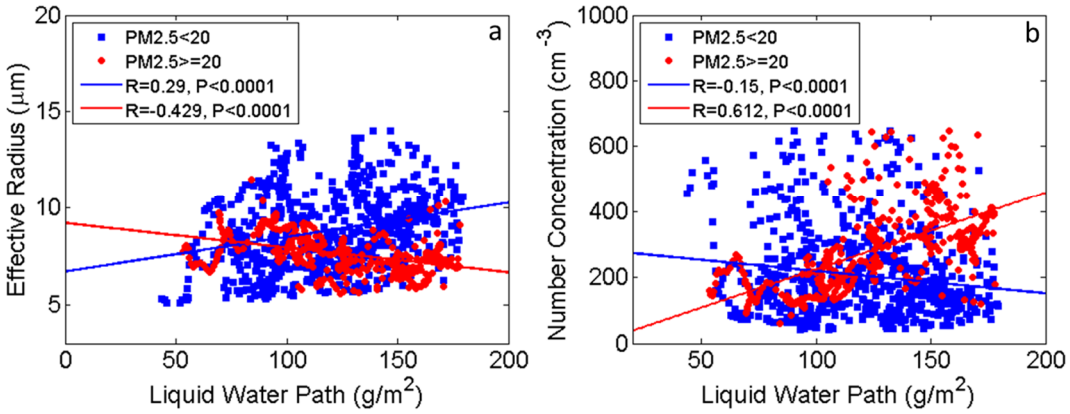

667

668 **Fig. 6.** (a) The relationship between Re and LWP under different PM2.5 value , and (b)
669 the relationship between cloud droplets number concentration and liquid water
670 path under different PM2.5 value.

671

672

673

674

675

676

677

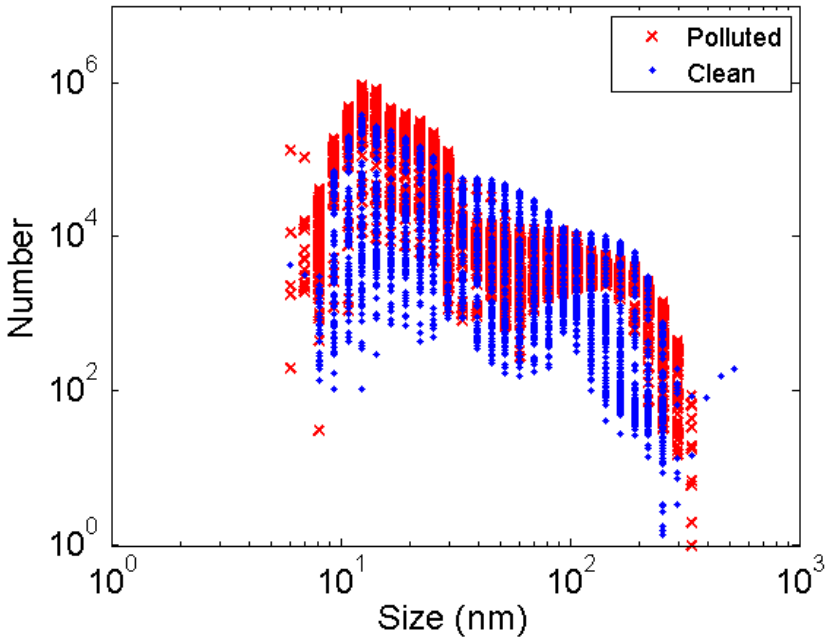

678

679 **Fig. 7.** FMPS measured aerosol size distribution on the polluted day (July 20th, 2011)
680 and clean day (July 14th , 2011) during DISCOVER AQ field campaign.

681

682

683

684

685

686

687

688

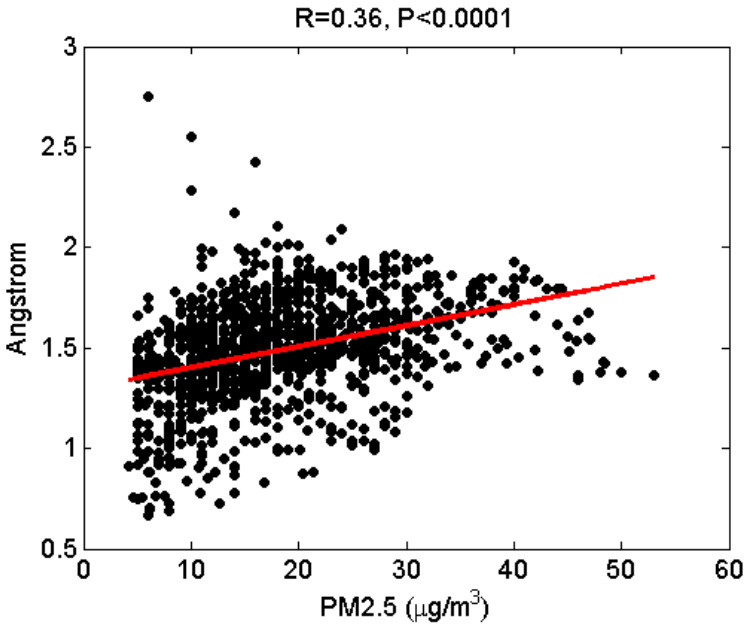

689

690 **Fig. 8.** The relationship of 5 years summer time hourly average Angstrom coefficient

691 and PM2.5.